

Virtual Arrays and Coarrays, Part 2: The Virtual Array

Mark A. Richards

August 2017

1 Array Antennas and Beam Patterns

In a previous technical memorandum [1] the antenna concepts of the phase center of an antenna and the virtual element (VE) associated with a transmit-receive (T-R) channel were discussed. We also introduced the notions of the far field and the parallel ray approximation. In this memo, we will build on these ideas to introduce the concept of the virtual array (VA), and to understand the virtues and limitation of the VA idea. Finally, we will show that various physical antenna array configurations and data collection protocols can generate useful VAs.

2 The Physical Configuration

Consider a radar system having a transmit (T) array antenna and a receive (R) array antenna. In general, the two are physically separate, though in many cases of interest they will be the same array. We assume both arrays are *compact* and that targets of interest are in the *far field* of each; see [1] for the definition of these terms. We also assume that the T and R arrays are *collocated*; this is as opposed to "widely separated" antennas. We are not aware of an accepted formal definition of the limit on T-R spacing that defines "collocated", but here we assume that spacing is much less than the distance to any scatterer \mathbf{P} of interest. While we could be more general, there is little of practical use to us to be gained by doing so.

Figure 1 illustrates the general configuration of interest [2]. A transmit array contains N_T elements at ranges R_{Tn} , $n = 0, \dots, N_T - 1$ from the scatterer \mathbf{P} and spans a total dimension of D_T . A receive array is similar, with N_R elements arranged over a total dimension D_R at ranges R_{Rn} , $n = 0, \dots, N_R - 1$ from \mathbf{P} . D_T and D_R are both much less than any of the $\{R_{Tn}\}$ and $\{R_{Rn}\}$ ("compact"), as is the separation between the T and R arrays ("collocated"). As a consequence of these assumptions, we can also assume that

- The parallel ray approximation is valid [1];
- The nominal angle from the transmit array to \mathbf{P} is approximately the same as that from the receive array to \mathbf{P} ;
- The nominal ranges from each array to \mathbf{P} are also approximately the same, so that ...
- The transmit and receive propagation losses are equal as well

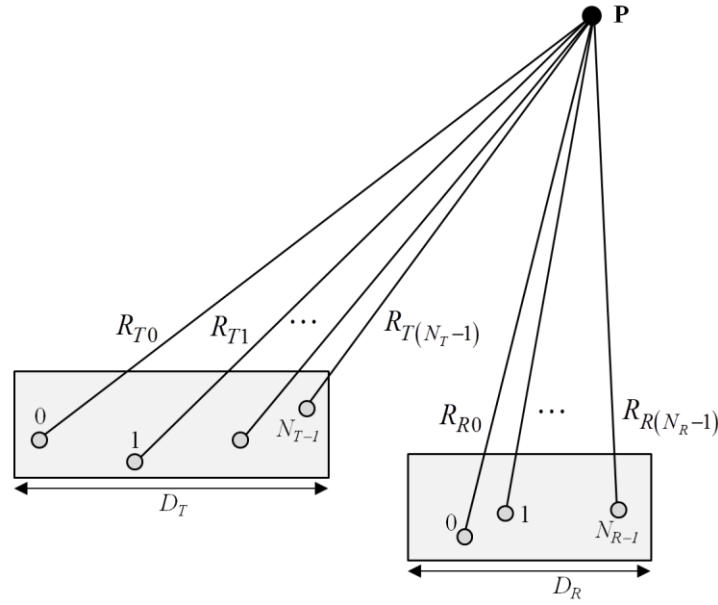


Figure 1. General compact, collocated transmit and receive arrays. The elements are not necessarily colinear or uniformly spaced, and the T and R arrays are not necessarily the same size.

If the signal $x(t) = A \exp[j(2\pi F_0 t + \phi_0)]$ is emitted from transmit element n ,¹ the complex amplitude \hat{A} of the signal at receive element m can be found from

$$\begin{aligned}
 x''(t) &= \rho \cdot k^2 \cdot x(t - (R_{Tn} + R_{Rm})/c) = \rho \cdot k \cdot A \cdot \exp\left[j\left(2\pi F_0 \left(t - (R_{Tn} + R_{Rm})/c\right) + \phi_0\right)\right] \\
 &= \rho \cdot k^2 \cdot A \cdot \exp\left[j(2\pi F_0 t + \phi_0)\right] \exp\left[-j(2\pi (R_{Tn} + R_{Rm})/\lambda)\right] \\
 &= \rho \cdot \hat{A} \exp\left[j(2\pi F_0 t + \phi_0)\right] \Rightarrow \hat{A} \equiv k^2 \cdot A \cdot \exp\left[-j(2\pi (R_{Tn} + R_{Rm})/\lambda)\right]
 \end{aligned} \tag{1}$$

Here ρ is the reflectivity of the scatterer \mathbf{P} . As in [1], k accounts for all amplitude factors due to one-way propagation, e.g. the $1/R$ amplitude loss and any atmospheric losses.

In this memo, we will be concerned primarily with one-dimensional linear arrays (LAs), often but not always shared for both transmit and receive, as shown in Figure 2. The left half of the figure shows a non-equispaced array of N elements. Let N be odd initially, $N = 2M + 1$, and index the elements from $-M$ to $+M$. Let the zero-indexed element be located at the origin on the x axis; note that this is not necessarily the center of the array extent D . The right half of the figure shows the common case of equispaced elements, called a *uniform linear array* (ULA). In this case the element locations are $x_n = nd$, the origin is at the center of the ULA, and the parallel ray approximation gives the range from each element to \mathbf{P} as $R_n = R_0 - nd \sin \theta$, $n = -M, \dots, +M$.

¹ When we eventually get to multiple-input, multiple-output (MIMO) radar, we will generalize further to allow different signals to be emitted from different transmit elements. But not yet.

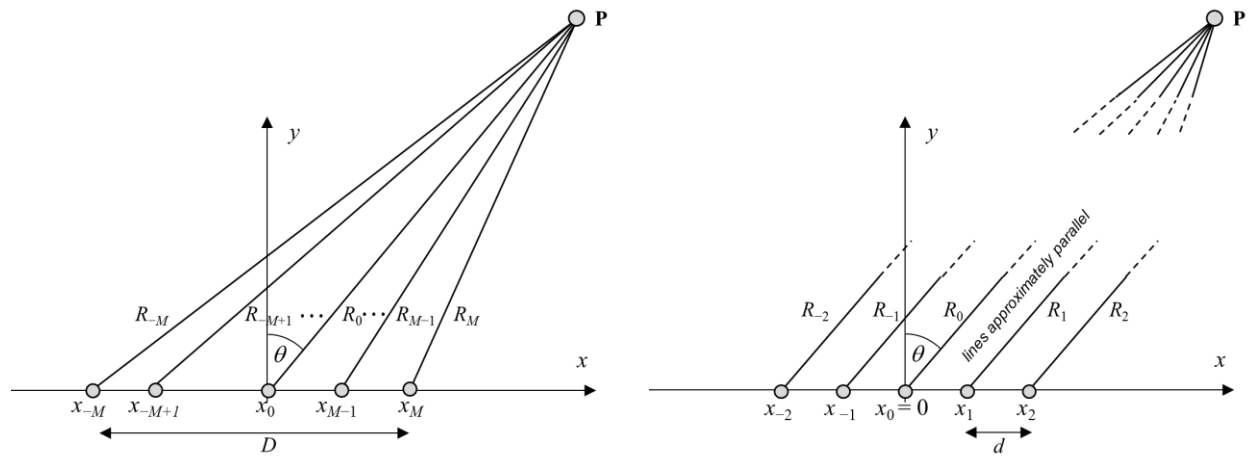


Figure 2. Compact one-dimensional linear arrays (LAs). In general, the elements are not uniformly spaced (left half of the figure). The uniform linear array (ULA) on the right has five equispaced elements indexed from -2 to $+2$ ($N = 5$, $M = 2$).

3 The Virtual Array

Given a transmit and receive array antenna, the corresponding *virtual array* (VA) is the assemblage of the virtual elements corresponding to each T-R channel [3][4]. In general, the VA will contain $N_R N_T$ VEs. Figure 3 illustrates the VA corresponding to the transmit and receive arrays of Figure 1. The left half of the figure shows the construction of the three VEs generated using the leftmost transmit element and the three receive elements; the VE is at the midpoint of the line connecting each T-R element pair. Also shown is the range from two of those VEs to \mathbf{P} . The right half shows the complete VA. The colors of the VEs that comprise the VA indicate the transmit element with which each is associated. There are $N_T N_R = 12$ T-R channels, and so 12 VEs in the VA.

Why is the virtual array useful? The VA defines a set of spatial sampling points such that a single monostatic VE at one of those points, transmitting and receiving the waveform $x(t)$, produces a received signal having the same complex amplitude that would be observed by transmitting and receiving using the actual T-R element pair that defined the channel represented by that VE. The output of the entire VA therefore defines the effective spatial sampling pattern with which the target environment has been probed and provides the phase histories of all the signal components present at the output of physical T-R array configuration.

While these are useful properties, we will see going forward that the VA does not by itself specify other important antenna system properties, specifically the gain, angular resolution and sidelobe structure.

For those we will need the physical array geometry.²

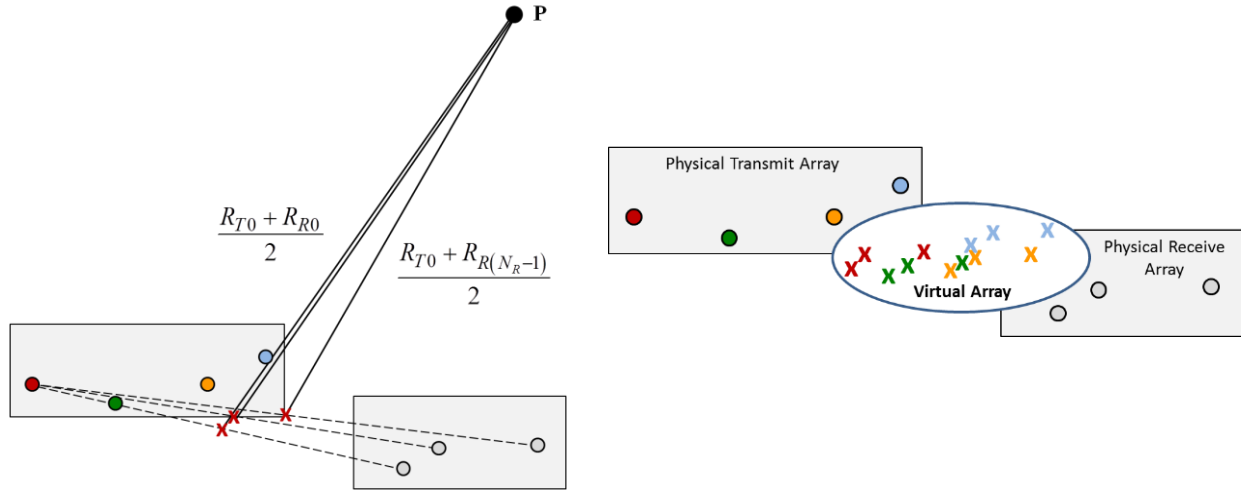


Figure 3. The virtual array. The left half of the figure illustrates construction of the location of the three virtual elements of the virtual array corresponding to the leftmost transmit element. The right half shows the complete virtual array. The colors indicate which VEs are associated with which transmit element.

4 The Effect of a Single Input

Consider the bistatic configuration with LAs for both transmit and receive shown in Figure 4. Assume that each of the transmit elements simultaneously transmits isotropically the *same* signal $x(t) = A \exp[j(2\pi F_0 t + \phi_0)]$. We call this *single input* (SI) operation.³ The received signal at **P** will be

$$\begin{aligned}
 x'(t) &= k \sum_{n=-M_T}^{M_T} x(t - R_{Tn}/c) = k \cdot A \cdot \exp[j(2\pi F_0 t + \phi_0)] \underbrace{\sum_{n=-M_T}^{M_T} \exp(-j2\pi R_{Tn}/\lambda)}_{\equiv CAF_T(\theta_T)} \\
 &= \hat{A}(\theta_T) \exp[j(2\pi F_0 t + \phi_0)], \quad \hat{A}(\theta_T) \equiv k \cdot A \cdot CAF_T(\theta_T)
 \end{aligned} \tag{2}$$

² Or, eventually the coarray, to be discussed in the next memo in this series [5]

³ This is also called the *phased array* case in the MIMO literature.

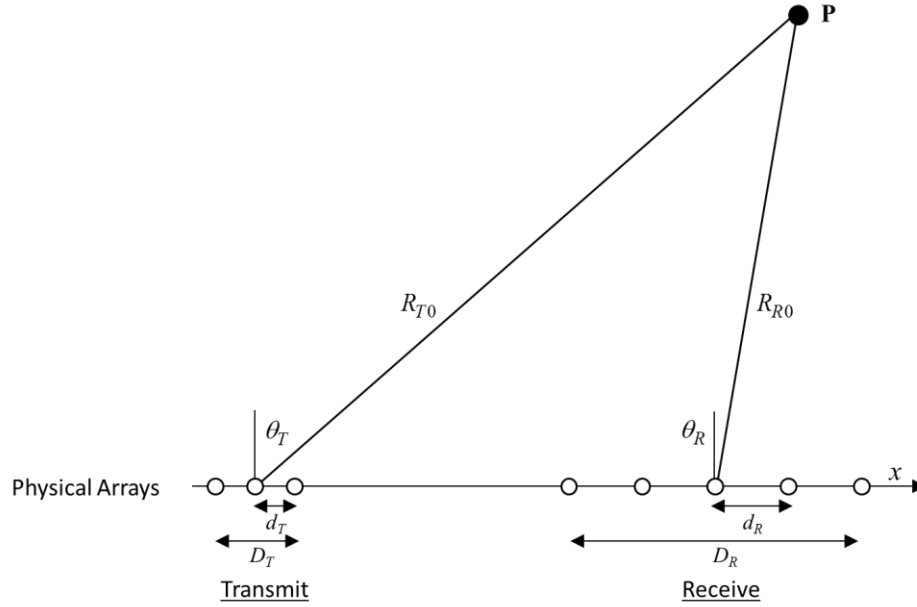


Figure 4. A 1D bistatic ULA configuration.

R_{Tn} is the range from the n^{th} transmit element to \mathbf{P} . We have assumed that N_T is odd, $N_T = 2M_T + 1$, and that n is indexed from $-M_T$ to $+M_T$. The summation involving the ranges is called the *complex array factor* (CAF). It is a function of the angle θ_T because the ranges R_{Tn} depend on θ_T . The CAF will determine the directive beam pattern of the transmit array and therefore the peak gain, mainlobe width, and sidelobe structure. However, the key point is that in SI operation the signal observed at \mathbf{P} is identical to that originating from a single element with complex amplitude $\hat{A}(\theta_T)$. Therefore, the transmit array can be replaced by a single virtual element at a range of $(-\lambda/2\pi)\arg[CAF_T(\theta_T)]$ and transmitting with an angle-dependent amplitude $|A \cdot CAF_T(\theta_T)|$. We also see that, since the effective transmit antenna is a single VE, the number of distinct channels in the T-R configuration is reduced from $N_T N_R$ to just N_R .

If the transmit array is a ULA, $R_{Tn} = R_{T0} - nd_T \sin \theta_T$ and the CAF becomes

$$\begin{aligned}
 CAF_T(\theta_T) &= \sum_{n=-M_T}^{M_T} \exp[+j2\pi(R_{T0} - nd_T \sin \theta_T)/\lambda] \\
 &= \exp(-j2\pi R_{T0}/\lambda) \sum_{n=-M_T}^{M_T} \exp[+j2\pi nd_T \sin \theta_T / \lambda] \\
 &= \exp(-j2\pi R_{T0}/\lambda) \frac{\sin(\pi N_T d_T \sin \theta_T / \lambda)}{\sin(\pi d_T \sin \theta_T / \lambda)}
 \end{aligned} \tag{3}$$

The ULA transmit CAF is seen to be composed of two factors: the phase shift term $\exp(-j2\pi R_{T0}/\lambda)$ due to the nominal range from the transmit array to the scatterer, and an "aliased sinc"⁴ (asinc) term. The asinc term is real-valued with a maximum amplitude of N_T at $\theta_T = 0$, although it does undergo sign reversals and thus 180° phase changes at its zero crossings. However, if we restrict our attention to the mainlobe region $|\theta_T| \leq \sin^{-1}(\lambda/N_T d_T)$, only the amplitude of the CAF varies with θ_T ; its phase is constant.

The beam pattern of the transmit array antenna is approximately the product of the array factor and the *element pattern* of the physical antenna elements [6]. Because we are considering those elements to be isotropic and therefore to have a unity (omnidirectional) element pattern, for our purposes it is sufficient to take the CAF as the major determinant of the beam pattern and therefore of such important metrics as mainlobe width (angular resolution), gain, and sidelobe levels. The asinc transmit CAF in Eq. (3) has a peak amplitude of N_T , a mainlobe Rayleigh (peak-to-first null) width of $\sin^{-1}(\lambda/D_T) \approx \lambda/D_T$ radians (assuming $D \gg \lambda$), and a peak sidelobe level of -13.2 dB relative to the mainlobe peak.

Notice that the transmit CAF cannot be specified with only knowledge of the transmit VA geometry and operation method. As we have seen, the transmit VA corresponding to a ULA physical transmit array is a single VE at the physical array center; but this is the same as the VA for a physical transmitter that actually consists of one transmitting element at that same location. In the first case the magnitude of the CAF is the asinc function of Eq. (3), while in the second it equals unity. This counter-example shows that two different physical arrays that have the same VA will not have the same CAF in general. Therefore, the VA geometry does not uniquely specify the CAF; the physical transmit array geometry must be known to compute it.

If N_T is even, a similar development shows that the ULA phase center is still at the center of the array, even though the center falls between elements. In both cases (N_T odd or even), this result is the consequence of having symmetric pairs of elements on each side of the array center contributing equal-amplitude but opposite-sign phase terms to the signal received at \mathbf{P} . In fact, we can generalize to say any 1D array that is symmetric about its midpoint will have its phase center at that midpoint. Generalizing even further, the same can be said of any 2D or 3D array symmetric about its midpoint in all axes. Note that these arrays are not required to be uniform, i.e. to have periodically-spaced elements, but merely symmetric.

5 Some Virtual Array Examples

The following subsections illustrate several VA examples. In all of these examples, we will restrict ourselves to uniform linear arrays for both transmit and receive, since most practical cases of interest to us fall into that class.

⁴ Also called a "digital sinc" (dsinc), "periodic sinc" (psinc), or "Dirichlet" function.

5.1 The Bistatic SI Case

Using the results above, we can describe the VA for the bistatic T-R configuration shown in the top line of Figure 5. The arrays are colinear 1D ULAs with $N_T = 3$ and $N_R = 5$. Single input operation is assumed so the transmit array is equivalent to a single transmit virtual element at its center, as shown in the middle line. This VE would transmit with a complex amplitude equal to the CAF of Eq. (3). The dashed lines show the transmit and receive VE pairs that combine to form the left- and rightmost virtual elements of the VA on the third line, located at the midpoint between those pairs. The same process with the remaining receive VEs yields the complete VA shown. Both the VE spacing and the size of the VA are one-half those of the physical receive array. The VA is centered halfway between the T and R array centers. The number of distinct channels is N .

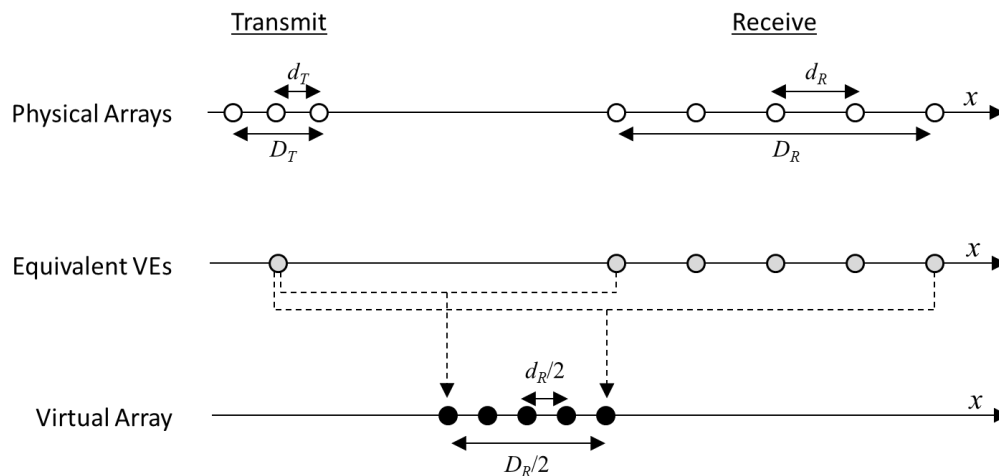


Figure 5. Physical and virtual arrays for a 1D bistatic ULA configuration.

5.2 The Monostatic SI Case

If the same physical array is shared for both transmit and receive, we have $N_T = N_R = N$, $d_T = d_R = d$, and $D_T = D_R = D$. The result is the same as the bistatic SI case, but with the VA centered at the same location as the physical array center. It is still the case that the VA is one-half the width of the physical array and that the number of distinct channels is only N .

5.3 Synthetic Aperture Radar

Synthetic aperture radar and sonar (SAR and SAS) is an imaging sensor technique for obtaining cross-range resolution much finer than can be obtained with a non-SAR or SAS “real beam” system. SAR concepts are discussed in [6]. Here, we are interested in the data collection protocol used by synthetic aperture sensors and the resulting virtual array.

A standard SAR system forms a synthetic array or aperture (SA) by physically locating a monostatic radar at one “element” location of the SA to be synthesized; radiating a pulse from that location; and

collecting and storing the received data vs. range. The radar (presumed carried on a moving platform such as an aircraft or spacecraft in SAR, or towed by a submarine or surface ship in SAS) then advances to the next "element" location in the SA and radiates and receives another pulse. This continues indefinitely, with the effective SA size being determined by a "sliding window" style of processing that combines data from N consecutive transmit locations to define the SA extent.

Figure 6 constructs the VA for this mode of operation. Since each pulse transmission consists of transmitting and receiving from the same physical location using only one "element"⁵, each such transmission defines a T-R channel whose virtual element is also at the same location. That is, the VA is simply the assemblage of transmit locations that will be combined in subsequent processing. The number of distinct channels is again N . The transmit CAF (from Eq. (3) with $M_T = 0 \rightarrow N = 1$) is independent of θ_T , i.e., omnidirectional:

$$CAF_T(\theta_T) = CAF_T = \exp(-j2\pi R_{T0}/\lambda) \tag{4}$$

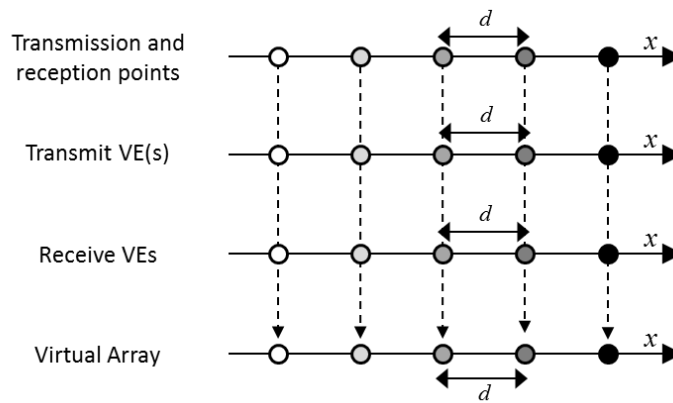


Figure 6. The virtual array in synthetic aperture operation. The shades of gray and dotted lines show which transmit and reception points define each virtual element in the VA.

It is well-known [6] that a standard synthetic array of size D produces a beamwidth half as wide as that of the physical phased array of the same extent, thus obtaining $2\times$ better angular resolution than the physical array. This is easily explained by comparing the VAs for the two cases. Consider Figure 7. The left half constructs the VA of a five-element single-input physical monostatic ULA. As discussed in Section 4, the phase center for transmission is the center of the array, resulting in a virtual array one-half the extent of the physical array.

⁵ The "stop and hop" approximation is usually invoked to justify ignoring motion of the platform during the pulse transit time. This is typically a very good assumption in SAR, less so in SAS. See [6] for a discussion.

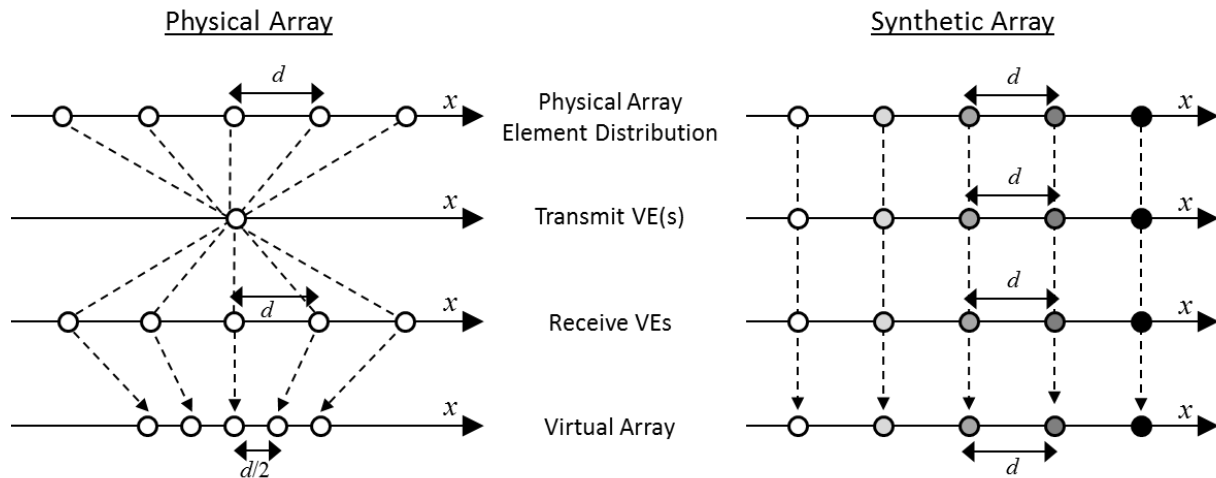


Figure 7. Virtual arrays for single-input physical and synthetic array formation. Dotted lines indicate which transmit and receive VE pairs form each VA element. Different shades of gray designate physical and virtual elements that correspond to the same pulse transmission: one pulse is transmitted in the physical array case, while five are transmitted in the synthetic array case.

The right half of the figure repeats the construction of Figure 6, resulting in a VA identical to the physical array. Therefore, the virtual array corresponding to a synthetic array of size D is twice the size of the VA corresponding to a physical array of the same size D . Assuming conventional sum beamforming, the larger VA explains the reduced beamwidth and improved angular resolution of the synthetic array over the physical array.

5.4 The Vernier Array

Figure 8 shows an example of using the virtual array concept to properly provide equispaced samples in the along-track dimension for a synthetic aperture system. The upper half of the figure shows a 4-element physical array where the rightmost element can both transmit and receive. Transmission occurs only from that element; the other three elements are receive-only. The figure shows the position of the physical array at three consecutive pulse transmission times. The sensor platform and array move to the right ($+x$ direction) only; the displacement in the vertical direction is just for convenience in illustrating the overlapped array positions at those three times. The bottom half of the figure shows that the consecutive positions of the half-sized VA provide continuous, equispaced sampling in the x dimension.

This mode of operation is sometimes called a *vernier array*. It is common in synthetic aperture sonar, where the slow speed of propagation of sound in water may make it impossible to maintain a platform velocity slow enough to receive the transmission from one pulse before another is needed at the next desired spatial sampling location unless the range swath is kept very small. The vernier array allows more platform motion between transmissions while maintaining adequate spatial sampling.

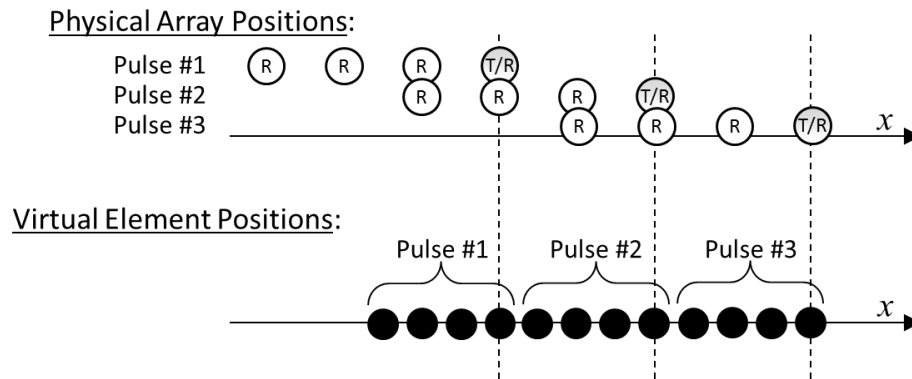


Figure 8. Operation of a physical SIMO arrays on consecutive pulses so as to provide continuous equispaced sampling. This technique is sometimes called a vernier array, and is common in synthetic aperture sonar.

5.5 Filling a Sparse Array

Figure 9 shows an example wherein a sparse physical array can result in a filled virtual array. The physical array has three transmitting elements which are operated separately; this is *not* a SI configuration. The colors of the virtual elements in the VA indicate the generating transmit element. The physical array is sparse in that it has no transmit or receive elements at the two locations with dashed circles. However, the resulting VA is *filled*, meaning that it has elements at uniform spacing with none missing. It is also non-redundant in that no two VEs exist at the same location. Thus, a filled VA can be created without the element cost of a completely filled physical array.

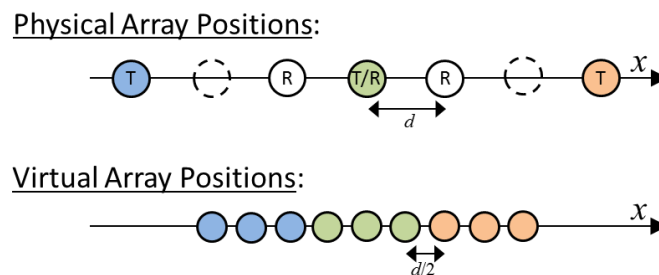


Figure 9. Creating a filled, non-redundant virtual array using a sparse physical array. The colors of the virtual elements in the VA indicate the generating transmit element.

6 The Effect of a Single Output

Many systems of practical interest are *single output* (SO) systems. In this memo, SO operation means that a sum beamformer is applied to the signals at each of the receive array outputs to form a single output for the array as a whole. The sum beamformer may be implemented either in microwave

hardware or digitally. We again restrict ourselves to linear arrays. In a manner identical to the analysis of SI operation in Section 4, it is easy to see that a linear receive array in SO operation is characterized by a complex array factor given by

$$CAF_R(\theta_R) = \sum_{n=-M_T}^{M_T} \exp(-j2\pi R_{Rn}/\lambda) \quad (5)$$

If the receive array is a ULA, $R_{Rn} = R_{R0} - nd_R \sin \theta_R$ the receive CAF becomes

$$CAF_R(\theta_R) = \exp(-j2\pi R_{R0}/\lambda) \frac{\sin(\pi N_R d_R \sin \theta_R / \lambda)}{\sin(\pi d_R \sin \theta_R / \lambda)} \quad (6)$$

The receive array can be represented with a single virtual element at a range of $(-\lambda/2\pi)\arg[CAF_R(\theta_R)]$ (R_{R0} in the ULA case) and exhibiting an angle-dependent gain $|CAF_R(\theta_R)|$. Single-output receive operation reduces the number of distinct channels in the T-R configuration from $N_T N_R$ to just N_T ; if the system is also SI, there is only one distinct channel.

It is common to apply an aperture weighting function $h[n]$ to the receive array elements.⁶ The general receive CAF then becomes

$$CAF_R(\theta_R) = \sum_{n=-M_T}^{M_T} h[n] \exp(-j2\pi R_{Rn}/\lambda) \quad (7)$$

In the ULA case, this is

$$\begin{aligned} CAF_R(\theta_R) &= \sum_{n=-M_T}^{M_T} h[n] \exp(-j2\pi(R_{R0} - nd_R \sin \theta_R)/\lambda) \\ &= \exp(-j2\pi R_{R0}/\lambda) \sum_{n=-M_T}^{M_T} h[n] \exp(+j2\pi nd_R \sin \theta_R / \lambda) \end{aligned} \quad (8)$$

With the substitution $n' = n - M$ and a redefinition of $h[n]$ to extend from $n = 0$ to $N_T - 1$ instead of from $-M_T$ to $+M_T$, this becomes

$$\begin{aligned} CAF_R(\theta_R) &= \exp[-j2\pi(R_{R0} + M_R d_R \sin \theta_R)/\lambda] \sum_{n'=0}^{N_T} h[n] \exp(j2\pi n' d_R \sin \theta_R / \lambda) \\ &= \exp[-j2\pi(R_{R0} + M_R d_R \sin \theta)/\lambda] H\left(\frac{d_R \sin \theta_R}{\lambda}\right)^* \end{aligned} \quad (9)$$

where $H(f)$ is the discrete-time Fourier transform (DTFT) of the weight sequence $h[n]$ [7]. The last

⁶ Although possible, it is much less common to do so on transmit because of the reduction in radiated power.

equality assumes that $h[n]$ is real-valued so that $H(f)$ exhibits conjugate symmetry. Thus, when receive weighting is used the receive CAF is, to within the overall phase constant, the complex conjugate of the DTFT of the weight function.

7 Two-Way Propagation with a Sum Beamformer: The Single Input, Single Output Array

Now assume SI transmission and consider reflection of the signal $x'(t)$ of Eq. (2) from \mathbf{P} to the receive array and the formation of a single output signal $x''(t)$ using a sum beamformer. (We assume uniform linear arrays, but it is easy to generalize to nonuniform LAs.) This combination of an SI transmit configuration with an SO receive beamformer is referred to here as a single-input, single-output or SISO array.⁷ Based on the preceding results, it is easy to see that the SISO output signal will be⁸

$$x_n''(t) = k^2 \cdot A \cdot \rho \cdot \exp[j(2\pi F_0 t + \phi_0)] \underbrace{CAF_T(\theta) \cdot CAF_R(\theta)}_{\equiv CAF_{TR}(\theta)} \quad (10)$$

We have assumed that the propagation loss factor k is the same on transmit and receive. Also, under our compact, collocated, and far field assumption we can also set $\theta_T = \theta_R = \theta$ and $R_{T0} = R_{R0} = R$. Equation (10) shows that in SISO operation the two-way CAF is the product of the transmit and receive CAFs, as would be expected.

These observations show that, in regard to the phase history of the data, coherent simultaneous transmission from an array and reception at the same array with a sum beamformer is equivalent to transmission and reception at a VE located at the array center. It is necessary to compute and examine the two-way CAF for the particular physical array geometry and weighting to determine the gain, mainlobe width, and sidelobe structure of the system.

In the monostatic ULA case $N_T = N_R = N$, $d_T = d_R = d$, and $CAF_{TR}(\theta)$ becomes the square of the CAF in Eq. (3) or (6) (if no weighting is used). It follows that

- The peak amplitude of the two-way CAF is N^2 .
- The two-way CAF phase within its mainbeam region is a constant $-4\pi R_0/\lambda$ radians.
- The Rayleigh mainlobe width of the two-way CAF remains $\sin^{-1}(\lambda/D) \approx \lambda/D$ radians.
- The peak sidelobe level of the two-way CAF is -26.4 dB below the mainlobe peak.

It is interesting to again compare the physical and synthetic array cases. SAR processing is a form of sum beamforming, so the receive CAF for both cases is the same. However, recall that the SAR system

⁷ The SISO case is often referred to as the phased array case in the MIMO literature.

⁸ The use of time-delay or phase steering to direct the transmit and/or receive mainlobes in directions other than normal to the array face does not change any of our conclusions regarding phase centers and virtual elements, so we do not specifically consider electronic steering of the array.

transmits from only one "element" at a time, so the transmit CAF is the omnidirectional pattern of Eq. (4). The two-way CAF then equals the receive CAF, given by Eq. (6). Therefore, in comparison to the physical SISO array, the synthetic aperture two-way CAF has the following properties:

- The peak amplitude of the two-way CAF is N . For the physical SISO array it was N^2 .
- The two-way CAF phase within its mainbeam region is a constant $-4\pi R_0/\lambda$ radians; this is the same as the physical array.
- The Rayleigh mainlobe width of the two-way CAF is $\sin^{-1}(\lambda/2D) \approx \lambda/2D$ radians. This is a factor of two narrower than the physical array.
- The peak sidelobe level of the two-way CAF is -13.2 dB below the mainlobe peak. For the physical array, it was -26.4 dB.

Thus the SA system provides better finer angular resolution by a factor of two, but with higher sidelobes and less gain. Both the reduced gain and the increased sidelobes are a result of having the focusing effect of the array only on receive, whereas in the physical array case it is present on both transmit and receive.

8 Vector Representation of the Complex Array Factor

In anticipation of eventually discussing MIMO radar, it will (I hope) prove convenient, or at least more compact, to express the complex array factor calculation in vector notation. Start by defining a "path phase" column vector⁹ for an arbitrary array configuration (similar to the T or R array in Figure 1) with $N = 2M + 1$ elements:

$$\mathbf{p} = [\exp(j2\pi R_{-M}/\lambda) \quad \exp(j2\pi R_{-M+1}/\lambda) \quad \cdots \quad \exp(j2\pi R_M/\lambda)]^T \quad (11)$$

Inspection of Eqs. (2) and (5) shows that the complex array factor for either SI transmit or SO receive operation can be expressed in the form

$$CAF(\theta) = \mathbf{p}^H \mathbf{1}_N = \mathbf{1}_N^T \mathbf{p}^* \quad (12)$$

where $\mathbf{1}_N$ is a column vector of N ones. (The last equality follows because $\mathbf{p}^H \mathbf{1}_N$ is a scalar and thus its own transpose.) This formulation is easily extended to include amplitude weighting of the transmitted element signals by the N -vector of weights \mathbf{h} :

$$CAF(\theta) = (\mathbf{h} \odot \mathbf{p})^H \mathbf{1}_N = \mathbf{1}_N^T (\mathbf{h} \odot \mathbf{p})^* \quad (13)$$

where the symbol \odot represents the Hadamard (element-by-element) product. The two-way CAF for combined SISO (phased array) operation, including weighting on receive, is just

⁹ More commonly called the *steering vector* in digital and adaptive beamforming and processing.

$$CAF_{TR}(\theta) = \underbrace{(\mathbf{h} \odot \mathbf{p}_R)^H \mathbf{1}_N}_{\text{receive CAF}} \underbrace{\mathbf{p}_T^H \mathbf{1}_N}_{\text{transmit CAF}} = \mathbf{1}_N^T (\mathbf{h} \odot \mathbf{p}_R)^* \mathbf{p}_T^H \mathbf{1}_N \quad (14)$$

Finally, note that in the ULA case where $R_n = R_0 - nd \sin \theta$,

$$\begin{aligned} (\mathbf{h} \odot \mathbf{p})^H \mathbf{1}_N &= \mathbf{1}_N^T (\mathbf{h} \odot \mathbf{p})^* = \sum_{n=-M}^M \left\{ h[n] \exp[j2\pi(R_0 - nd \sin \theta)/\lambda] \right\}^* \\ &= \exp(-j2\pi R_0/\lambda) \sum_{n=-M}^M h[n] \exp[j2\pi nd \sin \theta/\lambda] \end{aligned} \quad (15)$$

This is identical in form to Eq. (8), so it must be that

$$(\mathbf{h} \odot \mathbf{p})^H \mathbf{1}_N = \mathbf{1}_N^T (\mathbf{h} \odot \mathbf{p})^* = \exp[-j2\pi(R_0 + Md \sin \theta)/\lambda] H\left(\frac{d \sin \theta}{\lambda}\right)^* \quad (16)$$

Equation (16) merely shows the form that the DFT calculation of the CAF takes in vector notation.

9 Recap: What is the Virtual Array Good For, and What Is It Not?

Given a physical transmit and receive array pair, we have now seen that

- The corresponding virtual array describes the effective set of spatial locations at which the target phase history is sampled. That is, independently operating a monostatic T-R element at each of the VA element locations will provide the same set of phase measurements as the physical configuration.
- The VA concept can be used to analyze the phase history sampling patterns of specified T-R physical array configurations, or to design physical configurations that will provide desired sampling patterns.
- Virtual arrays are not unique. There can be more than one physical T-R array configuration that produces the same VA.
- The virtual array does not directly support the calculation of one- or two-way array factors, and thus of beam patterns; therefore it does not support calculation of antenna gains or of mainlobe widths and sidelobe patterns. Knowledge of the physical array geometry is still required to calculate these metrics.

10 Non-Uniform and Three-Dimensional Extension

Similar to earlier discussion, most of our conclusions are not limited to uniform or one-dimensional arrays. Any two- or three-dimensional array in which all of the elements occur in pairs symmetric about the same center point \mathbf{x}_0 will have a VE at \mathbf{x}_0 which is the array's phase center. If the array is symmetric but not uniform (the elements are not periodically spaced), its CAF will not be an asinc form and the peak transmit and receive gains may be less than a factor of N each, where N is the total number of

elements. However, the CAF can certainly be computed and will be expressible in general as the product of two terms: (1) a constant phase term dependent on the nominal range to a scatterer, and (2) a sum of cosines, one for each symmetric pair of elements. This form guarantees that the CAF has a constant phase except for sign reversals at its zeros (if it has any). The array gains can be determined as the peak amplitude of the CAF.

11 References

- [1] M. A. Richards, "Virtual Arrays and Coarrays, Part 1: Phase Centers and Virtual Elements", technical memo, Feb. 2017. Available at <http://www.radarsp.com>.
- [2] J. Li and P. Stoica, "MIMO Radar – Diversity Means Superiority", Ch. 1 in J. Li and P. Stoica, editors, *MIMO Radar Signal Processing*. Wiley, 2009.
- [3] K. W. Forsythe and D. W. Bliss, "MIMO Radar: Concepts, Performance Enhancements, and Applications", Ch. 2 in J. Li and P. Stoica, editors, *MIMO Radar Signal Processing*. Wiley, 2009.
- [4] M. Davis, "MIMO Radar", Ch. 4 in W. L. Melvin and J. A. Scheer, editors, *Principles of Modern Radar: Advanced Techniques*, SciTech Publishing, 2013.
- [5] M. A. Richards, "Virtual Arrays and Coarrays, Part 3: Coarrays", technical memo, date TBD. Available at <http://www.radarsp.com>.
- [6] M. A. Richards, *Fundamentals of Radar Signal Processing*, second edition. McGraw-Hill, 2014.
- [7] Alan V. Oppenheim and Ronald W. Schaffer, *Discrete-Time Signal Processing*, 3rd edition. Pearson, 2009.